# Hot-melt extruded filaments based on pharmaceutical grade polymers for 3D printing by Fused Deposition Modeling

Alice Melocchi[a], Federico Parietti[b], Alessandra Maroni[a], Anastasia Foppoli[a], Andrea Gazzaniga[a], Lucia Zema[a]*

[a]Università degli Studi di Milano, Dipartimento di Scienze Farmaceutiche, Sezione di Tecnologia e Legislazione Farmaceutiche "M.E. Sangalli", Via G. Colombo 71, 20133 Milan, Italy; alice.melocchi@unimi.it, alessandra.maroni@unimi.it, anastasia.foppoli@unimi.it, andrea.gazzaniga@unimi.it

[b]Massachusetts Institute of Technology, Mechanical Engineering Department, 77 Massachusetts Ave, Cambridge US-MA 02139; parietti@mit.edu

*Corresponding author: L. Zema; Telephone: +39-02-503-24654;

E-mail: lucia.zema@unimi.it

## Abstract

Fused deposition modeling (FDM) is a 3D printing technique based on the deposition of successive layers of thermoplastic materials following their softening/melting. Such a technique holds huge potential for the manufacturing of pharmaceutical products and is currently under extensive investigation. Challenges in this field are mainly related to the paucity of adequate filaments composed of pharmaceutical grade materials, which are needed for feeding the FDM equipment. Accordingly, a number of polymers of common use in pharmaceutical formulation were evaluated as starting materials for fabrication via hot melt extrusion of filaments suitable for FDM processes. By using a twin-screw extruder, filaments based on insoluble (ethylcellulose, Eudragit® RL), promptly soluble (polyethylene oxide, Kollicoat® IR), enteric soluble (Eudragit® L, hydroxypropyl methylcellulose acetate succinate) and swellable/erodible (hydrophilic cellulose derivatives, polyvinyl alcohol, Soluplus®) polymers were successfully produced, and the possibility of employing them for printing 600 μm thick disks was demonstrated. The behavior of disks as barriers when in contact with aqueous fluids was shown consistent with the functional application of the relevant polymeric components. The produced filaments were thus considered potentially suitable for printing capsules and coating layers for immediate or modified release, and, when loaded with active ingredients, any type of dosage forms.

**Keywords:** 3D printing, fused deposition modeling, hot melt extrusion, filament, pharmaceutical grade polymer, drug delivery system

## 1. Introduction

Some major challenges that still have to be faced in the field of drug delivery (*e.g.* drug targeting, administration of proteins, personalized therapy) and pharmaceutical production (*e.g.* continuous manufacturing, optimization) relate to the development and proper application of new manufacturing techniques, such as hot-processing including hot melt extrusion (HME), injection molding (IM) and 3D printing (3DP) by fused deposition modeling (FDM) (Maroni et al., 2012; Park, 2015; Mascia et al., 2013, Melocchi et al, 2015a; Norman et al., 2016; Shah et al., 2013; Zema et al., 2012). As far as 3DP is concerned, it has gained huge interest in recent years after finding widespread application in many industrial domains (*e.g.* automotive, aerospace, fashion and defense), where it is also exploited as a rapid prototyping tool. In this respect, it allows a representation of an item to be created before its final release or commercialization, thus reducing time and costs of the development. Moreover, 3DP turned out to be promising in the biomedical field for producing personalized prostheses on the basis of each patient's characteristics and needs, as identified by imaging techniques (*e.g.* x-ray computed tomography, nuclear magnetic resonance) (Rengier et al., 2010). 3DP includes a variety of techniques (*e.g.* stereolithography, selective laser sintering, fused deposition modeling). They all enable the fabrication of objects starting from digital models through the addition of successive layers (*i.e.* additive manufacturing), while differing in the starting materials and additive processes employed (Gibson et al. 2010; Pham and Gault, 1998).

3DP based on both powder solidification, first developed at Massachusetts Institute of Technology, and extrusion, was recently proposed for the development of drug products (Norman et al., 2016; Prasad and Smyth, 2015; Yu et al., 2008). Indeed, in 2015 the first 3D printed drug product (Spritam®) was approved by US Food and Drug Administration agency (FDA) (http://www.drugs.com/newdrugs/fda-approves-spritam-levetiracetam-first-3d-printed-product-4240.html; http://www.spritam.com). It is a tablet that can be loaded with differing doses (up to 1000 mg) of levetiracetam, manufactured through the Aprecia's ZipDose® technology. This exploits

3DP by powder solidification to produce a porous orodispersible formulation that rapidly disintegrates in a very low amount of liquid.

FDM is an extrusion-based 3DP technique easily accessible, low-cost, versatile and characterized by a good potential for fabrication of single-unit dosage forms (Goyanes et al., 2015a; Norman et al., 2016; Yu et al., 2008). It allows the type, dose, and distribution of the active ingredient as well as the size, shape, geometry (*e.g.* hollow, multi-layer, coated) and density of the final product to be varied, thus ideally meeting the needs of personalized medicine (Goyanes et al., 2015b and c; Melocchi et al., 2015b; Skowyra et al., 2015). FDM consists in the deposition, on a build plate, of molten/softened materials from a heated printer extrusion head that moves along the x and y axes, while lowering of the build plate enables the growth of the item bottom-up (Gibson et al., 2010). Starting materials are generally supplied in the form of filaments, which are produced by HME. The first commercially available filaments were mainly based on acrylonitrile butadiene styrene (ABS) and polylactic acid (PLA). Because of the increasing interest in FDM, the fabrication of filaments has become an important research area. Therefore, not only the use of other materials was explored, *e.g.* polyvinyl alcohol (PVA), XT copolyester, polyethylene terephthalate, nylon, thermoplastic polyurethane, but also different physical/mechanical properties of filaments (*e.g.* color, resistance, flexibility) were pursued. In the pharmaceutical field, early attempts were carried out using plastics (*e.g.* ethylene vinyl acetate, PLA, PVA) also in the form of filaments available on the market, introducing the active ingredient by soaking or extrusion (Genina et al., 2016; Goyanes et al., 2014; Goyanes et al., 2015a, b, c and d; Holländer, et al., 2016; Sandler et al., 2014; Skowyra et al., 2015; Water et al., 2015). Only very recently, a few drug-containing monolithic units intended for oral administration were described based on purposely-extruded filaments (Pietrzak at al., 2015). Moreover, starting from filaments based on hydroxypropyl cellulose (HPC), hollow items in the form of caps and bodies to be assembled in a capsule shell for pulsatile release were prepared (Melocchi et al., 2015b). FDM was also demonstrated a suitable prototyping tool for swellable/erodible capsular delivery platforms prepared by IM (Gazzaniga et al., 2011; Macchi et

al., 2015; Melocchi et al., 2015b; Zema et al., 2013a). However, few thermoplastic materials were investigated so far, none of which is commercially available as filaments. Hence, in view of the variety of polymeric materials used in the manufacturing of dosage forms and DDSs, investigations in this respect need to be broadened. The availability of libraries of polymeric filaments, which may differ in terms of physico-technological characteristics and processing conditions while allowing products with comparable performance to be obtained, could be of great interest, for instance to circumvent stability issues related to the operating temperatures involved by each material.

Based on these premises, the aim of the present work was to produce filaments suitable for FDM starting from a variety of pharmaceutical grade polymers having differing physico-chemical characteristics. Particularly, insoluble, promptly soluble, enteric soluble and swellable/erodible polymers were considered. Such filaments would be intended for fabrication of capsule shells and coatings for either immediate or modified release. In addition, they could be loaded with active ingredients and then employed for the manufacturing of printed monolithic drug products (*e.g.* pellets, tablets, matrices).

## 2. Materials and Methods

### 2.1 Materials

Polylactic acid, PLA filament (L-PLA natural, ø 1.75 mm; MakerBot® Industries, LLC, US-NY); ethyl cellulose, EC (Ethocel™ Std. 100 premium, Dow, US-MY); hydroxypropyl cellulose, HPC (Klucel® LF, Ashland, US-NJ); hydroxypropyl methyl cellulose, HPMC (Affinisol™ 15cP, Dow, US-CA); hydroxypropyl methyl cellulose acetate succinate, HPMCAS **(**AQUOT-LG®; Shin-Etsu, J); methacrylic acid copolymer Eudragit® L 100-55, EDR L, and Eudragit® RL PO, EDR RL (Evonik, D); polyethylene oxide, PEO (Sentry Polyox ™ WSR N10 LEO NF, Colorcon, UK); polyvinyl alcohol, PVA (Gohsenol® EG 05P, Nippon Goshei, J); polyvinyl alcohol-polyethylene glycol graft copolymer, KIR (Kollicoat® IR, BASF, D); polyvinyl caprolactam-polyvinyl acetate-polyethylene glycol graft co-polymer, SLP (Soluplus®, BASF, D); glycerol, GLY (Pharmagel, I); polyethylene glycols, PEG 400 and

PEG 8000 (Clariant Masterbatches, I); triethyl citrate, TEC (Sigma Aldrich, D); acetaminophen, AAP (Rhodia, I); furosemide, FUR (Metapharmaceutical, E).

## 2.2 Methods

PLA filament was used as received. All materials, except for PEGs, GLY, TEC, AAP and FUR, were kept in an oven at 40 °C for 24 h prior to use. Plasticized polymeric formulations were prepared by mixing polymers with the selected plasticizer in a mortar. The amount of plasticizer was expressed as % by weight on the dry polymer. FUR was added to the KIR-based formulation by mixing in a mortar and its amount was expressed as % by weight on the final mixture (*i.e.* 30%).

### *2.1.1 Preparation of filaments*

Filaments were prepared by HME using a twin-screw extruder (Haake™ MiniLab II, Thermo Scientific, US-WI) equipped with counter-rotating screws and a custom-made aluminum rod-shaped die (ø = 1.80 mm); process conditions are reported in the Results section. Extruded rods were manually pulled and forced to pass through a caliber connected with the extruder and set at 1.80 mm. After production, filament diameter was verified every 5 cm in length and portions that had not diameter in the acceptable range of 1.75 ± 0.05 mm were discarded.

### *2.1.2 Printing of disks*

FDM was performed by an adapted MakerBot Replicator 2 equipped with a 0.4 mm tip (MakerBot® Industries, US-NY; infill = 100%, layer height = 0.30 mm), using a computer-aided design (CAD) file purposely developed. In particular, a disk (ø = 30 mm and thickness = 600 µm) was designed using Autodesk® Autocad® 2016 software version 14.0 (Autodesk, Inc., US-CA), saved in STL format and imported to the 3D printer software (MakerWare Version 2.2.2.89, MakerBot® Industries, US-NY). Either the supplied PLA filament or portions of at least 25 cm of the in-house prepared filaments were employed.

The printing temperature was adapted to the thermal and mechanical behavior of each material. When changing the filament before a new printing process, the printer was cleaned and leveling of the build plate was performed following assembly of the heating chamber. Cleaning procedure: the temperature of the heating chamber was set at 250 °C for 3 min; then it was dismounted and the material remaining in the inner barrel was removed by means of a brass brush. In particular, the nozzle was unscrewed and any residue inside was manually removed; then it was immersed for at least 3 h in a suitable solvent depending on the solubility characteristics of the last printed material (*e.g.* water for KIR and PEO, acetone for PLA).

*2.1.4 Characterization of disks*

Disks were stored between plates before being characterized in terms of weight (analytical balance BP211, Sartorius, D; n = 6) and thickness (MiniTest FH7200 equipped with FH4 probe, ø sphere = 1.5 mm, ElektroPhysik, D; n = 6), in order to avoid warpage phenomena. Digital photographs of samples were acquired (Dino Lite Digital Microscope coupled with Dino Capture software, Dino-Lite, VWR International, I).

Thickness was measured in 6 points for each of 3 concentric circumferences (Figure 1). Radius was of 4mm, 7.5 mm and 13 mm for the inner, intermediate and outer circumference, respectively. Values were reported as mean and the coefficient of variation (CV) was calculated.

Mass loss test was carried out by a six-position disintegration apparatus (900 mL of distilled water for KIR, HPC, HPMC, PVA, SLP and EDR RL disks; 2 h in HCl 0.1 N and then pH 6.8 phosphate buffer, according to Dissolution test for delayed-release dosage forms, Method B, USP 38, for EDR L and HPMCAS disks; 37 ± 0.5 °C; 31 cycles/min). Before testing, disks were die-cut into smaller ones (ø = 11 mm) and each of them was checked for weight (initial weight, $w_i$) and inserted into a single basket-rack assembly. At pre-determined time points, samples (n = 3) were withdrawn, gently blotted and weighed (wet weigh, $w_w$). Final dry weights ($w_d$) were then determined after oven-

drying (40 °C) to constant weight. The water uptake percentage (% WU) and residual dry mass percentage (% RDM) were calculated according to the following equations:

$$\% WU = \left[\left(\frac{w_w - w_d}{w_w}\right) \times 100\right] \quad \text{eq. 1}$$

$$\% RDM = \left[\left(\frac{w_d}{w_i}\right) \times 100\right] \quad \text{eq. 2}$$

Disks were also tested for barrier performance (n = 3). For this purpose, they were mounted to close manually-assembled cells (area exposed to the medium = 177 $mm^2$) (Figure 2) (Zema et al., 2013b). When testing polymeric disks the donor reservoir compartment was filled with 100 mg of AAP powder as a tracer (Giordano et al., 2005). The test was performed in a USP 38 dissolution apparatus 2 (Dissolution System 2100B, Distek, US-MA; 900 mL of medium, 100 rpm, 37 ± 0.5 °C). Fluids were the same as for the mass loss test. Fluid samples were withdrawn at fixed time points and drug was assayed by spectrophotometer (Lambda25, Perkin Elmer, US-MA; 254 nm). The time to 10% recovery from the acceptor fluid ($t_{10\%}$) was calculated by linear interpolation of the experimental data immediately before and after this release %. In the case of enteric-soluble polymers $t_{10\%}$ was calculated after the pH change.

$t_{10\%}$ data relevant to swellable/erodible polymer barriers were used to calculate the time equivalent thickness parameter (TETP) according to the following equation (Sangalli et al., 2004):

$$TETP = \frac{disk\ thickness}{t_{10\%}}$$

where disk thickness is the mean of values measured along the inner and central circumferences (n = 12), in order to consider the surface exposed to the medium only. This parameter expresses the thickness of the barrier (μm) needed to attain a unit of lag time (min).

Disks containing FUR and double-disk items were mounted to close the above-mentioned cells, wherein the donor reservoir compartment was left empty. The test was performed in a USP 38 dissolution apparatus 2 (Dissolution System 2100B, Distek, US-MA; 1000 mL of medium, 100 rpm, 37 ± 0.5 °C), under sink conditions. The FUR-containing disk was tested in pH 6.8 phosphate buffer, while the fluids used to test double-disk items were in those indicated in the Dissolution test for delayed-release dosage forms, Method B, USP 38. Fluid samples were withdrawn at fixed time points and drug was assayed by spectrophotometer (Lambda25, Perkin Elmer, US-MA; 274 nm).

## 3. Results and Discussion

### 3.1 Extrusion of filaments and printing of disks

A variety of pharmaceutical grade polymers with different functional applications and a potential for hot-processing was selected for the manufacturing of filaments by HME. In particular, the use of a number of promptly soluble (*i.e.* KIR, PEO), enteric soluble (*i.e.* HPMCAS, EDR L), swellable/erodible (*i.e.* HPC, HPMC, PVA, SLP) and insoluble (*i.e.* EC, EDR RL) selected polymers was explored.

The formulation and processing conditions that would allow filaments suitable for feeding a commercially-available FDM equipment were investigated. A desktop, user-friendly printer, MakerBot Replicator 2, designed to work with PLA filaments and equipped with a standard 0.4 mm tip, was employed for 3DP processes. Disk-shaped items of 600 μm in thickness were identified as viable specimens for the screening of materials. Indeed, though requiring a simple CAD file to be designed, they could both highlight challenges in filament deposition on account of the limited thickness/diameter ratio, and provide preliminary information on the achievable performance. Notably, the possibility of producing thin items having narrow thickness tolerance ranges is of utmost importance in the pharmaceutical field, especially for the manufacturing of coated dosage forms or capsular devices.

In order to explore the feasibility of items having such features, initial trials were performed using the supplied Makerbot PLA filament and standard printing conditions in compliance with the technical specifications of the equipment. Based on the CAD file developed, the disks were automatically fabricated through the addition of two successive layers, the latter being deposited onto the former perpendicularly on the horizontal plane as envisaged by the 3D printer software.

Prior to each printing step, the build plate needs to be manually levelled, by setting its distance from the nozzle. Because this operation appeared potentially critical to the vertical growth of the object, its impact on consistency of the disk thickness was evaluated. Accordingly, 3 leveling replicates by 2 different operators were undertaken. After each of them, a batch of 6 disks was produced. The disks were characterized in terms of weight and thickness, the latter being measured along 3 concentric circumferences (Table 1). For each leveling replicate, the mean disk weight (n = 6) and the mean disk thickness from the measurements either along each circumference (n = 6) or all the 3 circumferences (n = 18) were calculated, in order to gain information on intra-operation variability. In addition, mean weight and thickness values were calculated considering all samples from different batches (n = 36) in order to also take inter-operation variability into account.

Good results in terms of continuous flow of the material from the nozzle during the printing process were indicated by the low weight variability (CV < 2). However, thickness data poorly complied with the value defined in the CAD file (*i.e.* 600 µm) and showed reproducibility issues. In particular, intra-operation differences (*i.e.* among disks printed following the same leveling) up to about 200 µm and inter-operation differences (*i.e.* among disks printed following 2 different levelings) up to about 400 µm were observed. Because disks are composed of 2 layers only, leveling, which determines the thickness of the former layer by establishing the distance between the nozzle and the build plate, ultimately affects the final thickness. Moreover, these results highlighted inherent resolution limits of the printer, used under standard operating conditions (*e.g.* PLA filament and 0.4 mm tip), which would have to be taken into account when the quality standards of pharmaceutical products need to be fulfilled.

With regard to the extrusion of filaments from the selected pharmaceutical grade polymers, the type and amount of plasticizers were adjusted, based on the torque values recorded, to enable continuous extrusion throughout the barrel of the employed equipment that has limited length (12 cm). This would indeed result in relatively short-lasting exposure of the material to the temperature and shear stress conditions that cause its softening/melting. Previous 3DP trials pointed out the need for filaments with a minimum length of 25 cm, circular cross section and proper diameter as well as diameter tolerances (1.75 ± 0.05 mm) (Melocchi et al., 2015b). For the purpose of producing suitable filaments, the twin-screw extruder used was equipped with a custom-made aluminum die having a conical section at the entry side and a cylindrical section at the exit. The extruded filaments were then pulled manually through a gauge of 1.80 mm to maintain the desired diameter. The size of filaments, checked every 5 cm, turned out slightly lower than the PLA one (mean = 1.71 mm, CV 2.30 *vs* 1.79 mm, CV 1.10). Not only the diameter but also the mechanical properties of the filament were critical to 3DP processability. Problems of rupture or wrapping around gears were initially encountered. In order to overcome these issues, the feeding mechanism of the printer was modified by replacing the standard spring with one of lower stiffness, thus reducing the compression force applied and possibly broadening the range of formulations that could be used. When feeding failure still occurred, small increases or decreases in the amount of plasticizer (1%), depending on whether rupturing or wrapping problems had to be faced, respectively, were systematically attempted. This trial and error approach was continued until formulations suitable for both extrusion of filaments and feeding of the printer were attained.

The formulation and the extrusion as well as FDM processing conditions relevant to each polymer investigated, along with photographs of the extruded filaments and printed disks, are reported in Table 2.

The temperature needed for printing generally turned out to be higher than for extrusion of filaments. This may be due to the short residence time of the material in the heating chamber of the 3D printer and, also, to the limited contribution of the shear stress developed by the loading gear, if

compared with the counter-rotating tween-screws of the extruder. Problems of nozzle clogging following increase in the melt viscosity, caused by decrease in the FDM processing temperature, were already described (Pietrzak at al., 2015). Moreover, because an unheated build plate was used, as involved by the standard configuration of Makerbot Replicator 2, the temperature of the material flowing out from the heating chamber also needed to compensate for the sudden cooling occurring on deposition, which could hinder proper adherence of the layers to each other and to the surface of the plate. Removal of disks from the build plate without damaging was in all cases possible because of sufficient cohesion between the overlapping layers. The extent of plasticization was found critical in this respect.

The printing process took approximately 2 min per disk. Entire printed disks were obtained, wherein the 90° deposition pattern was evident (Table 2). When trying to improve the printing resolution, disks with the required physico-technological characteristics were not always obtained. High-resolution setting necessarily involves decreased rate of deposition and reduced layer thickness, and this may have worsened issues related to sudden cooling of the melt.

Weight and thickness data of disks are reported in Table 3.

The variability of both weight and thickness turned out increased with respect to disks printed from the Makerbot supplied PLA filament though using the same CAD file. Moreover, the average thickness of the disks based on pharmaceutical grade polymers was generally lower than the nominal value, ranging from less than 500 μm to approximately 600 μm. Such results were partly expected due to the inherent characteristics of each material, such as the rheological behavior when melt and the possible tendency to volumetric changes after hot-processing (Zema et al., 2013a), and could also be ascribed to problems of continuous loading of the equipment. These would depend on the variability in diameter of the filaments produced in-house and their mechanical properties. Besides, such filaments were thinner than the supplied PLA one, ranging on average from 1.70 mm to 1.74 mm in diameter, which would impact on the thickness of the printed layers, especially when considering that the 3D printer is set for a filament of 1.77 mm in diameter. It should be noted that,

296 the possibility of modifying the CAD file to account for the volumetric changes of the material
297 following printing was already exploited with HPC (Melocchi et al., 2015b).
298
299 **3.2 Evaluation of the barrier performance of printed disks**

300 Disks were used as a simple model to evaluate the performance of printed barriers when in contact
301 with aqueous fluids, *i.e.* coatings and capsule shells. For this purpose, the disks were positioned to
302 close purposely-developed cells with a donor compartment that was filled with a drug tracer (Zema
303 et al., 2013b). The assembled cells were immersed in an acceptor medium and tests were carried out
304 in a dissolution apparatus 2. By assaying the drug recovered in the medium over time, cumulative
305 curves were obtained.
306 The behavior of disks based on promptly soluble polymers (*i.e.* KIR and PEO) was first explored
307 (Figure 3). With either polymeric barriers the whole amount of drug was found in the acceptor
308 medium after 15 min of testing. A further improvement in terms of dissolution rate could be
309 achieved by reducing the disk thickness. The dissolution of disks was rapidly completed after their
310 rupturing occurring within 5 and 10 min in the case of KIR and PEO, respectively. Also, mass loss
311 tests, carried out under different hydrodynamic conditions, showed that the printed samples based
312 on both materials entirely dissolved in 3 min. According to these results, KIR and PEO could be
313 employed as main components of coatings or capsules for immediate-release fabricated by FDM.
314 These printed capsules could represent an alternative to the gelatin and HPMC ones currently
315 available.
316 Disks based on the swellable/erodible polymers under investigation displayed the expected delay
317 prior to recovery of the drug tracer in the acceptor medium. Indeed, during the test they showed the
318 typical swelling and erosion/dissolution phenomena upon hydration, until break-up of the barrier.
319 After this lag phase, a fast increase in the amount of drug recovered in the medium was observed.

320 Such a pattern is typical of DDSs for pulsatile release. By way of example, individual profiles
321 relevant to HPMC-based disks are shown in Figure 4.
322 The curves presented are characterized by different lag times ($t_{10\%} \approx 65$, 75 and 85 min). Such
323 differences would at least partly be due to the diverse thickness values of each sample, *i.e.* 482 μm
324 (CV 7.6); 582 μm (CV 6.1), 603 μm (CV 3.2). The influence of the barrier thickness and of the
325 physico-chemical properties of the selected polymers on lag time is well-known and has largely
326 been demonstrated in the case of swellable/erodible reservoir systems prepared by IM, film-coating,
327 powder-layering and compression coating (Del Curto et al., 2014; Gazzaniga et al., 2011; Maroni et
328 al., 2013a and b; Maroni et al., 2016; Sangalli et al., 2009; Zema et al., 2013a). In order to compare
329 printed disks based on the various polymers investigated, a previously introduced index was
330 employed, the time equivalent thickness parameter (TETP), which expresses the thickness of a
331 polymeric layer needed to attain a lag time of 1 min (Table 4) (Sangalli et al., 2004). As expected,
332 TETP values pointed out a different efficiency of these polymers. The behavior of printed disks
333 based on SLP, purposely developed for the achievement of solid dispersions of poorly-soluble
334 drugs by HME, was comparable with that of barriers based on swellable polymers of established
335 use in the manufacturing of DDSs for pulsatile release.
336 The overall results pointed out the availability of a number of hydrophilic polymers other than HPC
337 that could be suitable for printing capsule shells and for modulating the onset of drug release
338 (Melocchi et al., 2015b).
339 From EC and EDR RL, poorly-permeable insoluble disks were obtained. Indeed, the amount of
340 drug recovered in the acceptor fluid increased very slowly, particularly when dealing with the EC
341 barrier (Figure 5). In this respect, although hot-processing techniques are known to lead to high-
342 density structures, FDM may grant the possibility of achieving different porosity characteristics
343 based on printing parameters, such as primarily on how close the layers are deposited (Loreti et al.,
344 2014; Melocchi et al., 2015a). The addition of channeling agents into the filament formulation may
345 also enhance the barrier permeability. The low rate of drug permeation could also be attributed to

346 the relatively high thickness of the printed disks as compared with films commonly applied to solid
347 dosage forms in order to prolong the drug release over time. Fabrication of thinner barriers, which
348 would most likely be intended for using as coatings rather than capsule shells, could represent a
349 further strategy to achieve release rates consistent with the oral administration route.
350 Finally, the barriers based on enteric soluble polymers, *i.e.* HPMCAS and EDR L, were evaluated
351 by using HCl 0.1 N and then phosphate buffer pH 6.8 as the acceptor fluids. The disks showed the
352 expected resistance when in contact with the acidic medium. When switching to phosphate buffer, a
353 lag time elapsed before dissolution and consequent rupture of the barriers. Such lag time was of
354 40.42 min (CV 7.32) and 45.95 min (CV 12.23) with HPMCAS and EDR L, respectively. From
355 HPMCAS-based disks and capsular devices manufactured by IM, a lag time before dissolution of
356 the enteric soluble polymer was analogously observed (Zema et al., 2013b). In that case, the time
357 taken for this process was shortened by adding channeling agents and/or reducing the thickness of
358 molded barriers, which could also be exploited with 3D printed items.
359

360 **3.3 Printing and evaluation of double-disk items**

361 In order to preliminarily evaluate the feasibility of FDM in the fabrication of coated dosage forms, a
362 double-disk item was obtained by successively printing two overlaid disks of different composition,
363 with no need for a newly designed CAD file. The filament for the former disk was extruded starting
364 from the KIR-based formulation containing furosemide (30% by weight), a poorly-soluble active
365 ingredient having high-melting point. The hot-processability of this model drug was already
366 demonstrated when mixed with the same polymer (Melocchi et al., 2015a). The latter disk was
367 based on HPMCAS.
368 The impact of the drug on the process parameters and quality of the product was negligible not only
369 as regards HME, as expected on the basis of previous experience, but also in the case of FDM.
370 After printing of the former disk, the remainder of the material was completely removed from the

heating chamber of the 3D printer by a purge operation before feeding the latter filament, which required to be processed at a higher temperature. Re-leveling was then performed with respect to the printed furosemide-containing disk. At the end of the process, the two parts of the double-disk item tightly adhered to each other, and the overall thickness was of 1052 μm (CV 12.7). For comparison purposes, single-disks containing furosemide were also printed.

Double-disk items were positioned into the cells for evaluation of performance, so that the enteric-soluble side was in contact with the medium and the drug-containing one was oriented towards the empty donor compartment. During the acidic stage of the test no drug was recovered in the acceptor medium, thus indicating that gastroresistance was effective (Figure 6). In the pH 6.8 fluid, the drug was released after a lag phase ($t_{10\%}$ = 49.06 min, CV 6.26) that turned out comparable in duration with that previously assessed when testing the HPMCAS disks as such. Moreover, the release pattern after the lag phase was analogous to that obtained from single furosemide-containing disks. These are the typically results that are observed from enteric-coated dosage forms.

## 4. Conclusions

Filaments based on a variety of pharmaceutical grade polymers, *i.e.* Kollicoat® IR, PEO, HPC, HPMC, PVA, Soluplus®, EC, Eudragit® RL, Eudragit® L and HPMCAS, were successfully produced, which turned out suitable for 3D printing by FDM. From filaments based on all these materials, disk-shaped specimens having thickness on the order of hundreds of microns were obtained. The printed disks were proved advantageous to investigate both the processability of the polymers and their behavior in contact with aqueous fluids after processing. When used as barriers, such disks performed as promptly-soluble, swellable/erodible, slowly-permeable insoluble and gastroresistant layers, consistent with the nature of their polymeric components and main applications in pharmaceutical formulation. Moreover, multiple overlaid disks were shown feasible. Overall, the potential of the investigated materials when processed by FDM was demonstrated for the manufacturing of immediate-release capsules, delivery platforms based on capsular devices and

cosmetic or functional coating layers. In addition, a variety of further products, such as tablets and matrices, could be obtained by incorporating active ingredients into the filaments.

As occurred in the past when transferring other industrial technologies to the pharmaceutical field (*e.g.* pelletization, HME, IM), a full exploitation of FDM and relevant broad application in this area actually require the development of suitable equipment and processes, which would enable the manufacturing of products complying with the strict quality standards involved.

## 5. References


Del Curto M. D., Palugan L., Foppoli A., Zema L., Gazzaniga A., Maroni A., Erodible time-dependent colon delivery systems with improved efficiency in delaying the onset of drug release, J. Pharm. Sci., 103: 3585-3593 (2014).

Gazzaniga A., Cerea M., Cozzi A., Foppoli A., Maroni A., Zema L., A novel injection-molded capsular device for oral pulsatile delivery based on swellable/erodible polymers, AAPS PharmSciTech., 12: 295-303 (2011).

Genina N., Holländer J., Jukarainen H., Mäkilä E., Salonen J., Sandler N., Ethylene vinyl acetate (EVA) as a new drug carrier for 3D printed medical drug delivery devices, Eur. J. Pharm. Sci., http://dx.doi.org/10.1016/j.ejps.2015.11.005 (2016).

Gibson I., Rosen D. W., Stucker B., Additive Manufacturing Technologies: rapid prototyping to direct digital manufacturing, Springer, New York (2010).

Giordano F., Rossi A., Bettini R., Savioli A., Gazzaniga A., Novák Cs., Thermal behavior of paracetamol polymeric excipients mixtures, J. Therm. Anal. Calorim., 68: 575-590 (2002).

Goyanes A., Buanz A. B. M., Basit A. W., Gaisford S., Fused-filament 3D printing (3DP) for fabrication of tablets, Int. J. Pharm., 476: 88-92 (2014).

Goyanes A., Robles Martinez P., Buanz A., Basit A. W., Gaisford S., Effect of geometry on drug release from 3D printed tablets , Int. J. Pharm., 494: 657-663 (2015a).

Goyanes A., Chang H., Sedough D., Hatton G. B., Wang J., Buanz A., Gaisford S., Basit A. W., Fabrication of controlled-release budesonide tablets via desktop (FDM) 3D printing, Int. J. Pharm., 496: 414-420 (2015b).

Goyanes A., Wang J., Buanz A., Martínez-Pacheco R., Telford R., Gaisford S., Basit A. W., 3D Printing of medicines: engineering novel oral devices with unique design and drug release characteristics, Mol. Pharm., 12: 4077-4084 (2015c).

Goyanes A., Buanz A. B. M., Hatton G. B., Gaisford S., Basit A. W., 3D printing of modified-release aminosalicylate (4-ASA and 5-ASA) tablets, Eur. J. Pharm. Biopharm., 89: 157-162 (2015d).

Holländer J., Genina N., Jukarainen H., Khajeheian M., Rosling A., Mäkilä E., Sandler N.,Three-dimensional printed PCL-based implantable prototypes of medical devices for controlled drug delivery, J. Pharm. Sci., doi:10.1016/j.xphs.2015.12.012 (2016).

http://www.drugs.com/newdrugs/fda-approves-spritam-levetiracetam-first-3d-printed-product-4240.html (accessed on 04/05/2016).

http://www.spritam.com (accessed on 04/05/2016).

Loreti G., Maroni A., Del Curto M. D., Melocchi A., Gazzaniga A., Zema L., Evaluation of hot melt extrusion technique in the production of HPC matrices for prolonged release, Eur. J. Pharm. Sci., 52: 77-85 (2014).

Macchi E., Zema L., Maroni A., Gazzaniga A., Felton L. A., Enteric-coating of pulsatile-release HPC capsules prepared by injection molding, Eur. J. Pharm. Sci., 70: 1-11 (2015).

442 Maroni A., Zema L., Del Curto M. D., Foppoli A., Gazzaniga A., Oral colon delivery of insulin
443 with the aid of functional adjuvants, Adv. Drug Deliv. Rev., 64: 540-556 (2012).

444 Maroni A., Zema L., Loreti G., Palugan L., Gazzaniga A., Film coatings for oral pulsatile release,
445 Int. J. Pharm., 457: 362-371 (2013a).

446 Maroni A., Del Curto M. D., Zema L., Foppoli A., Gazzaniga A., Film coatings for oral colon
447 delivery, Int. J. Pharm., 457: 372-394 (2013b).

448 Maroni A., Zema L., Cerea M., Foppoli A., Palugan L., Gazzaniga A., Erodible drug delivery
449 systems for time-controlled release into the gastrointestinal tract, J. Drug Deliv. Sci. Technol., 32:
450 229-235 (2016).

451 Mascia S., Heider P. L., Zhang H., Lakerveld R., Benyahia B., Barton P. I., Braatz R. D., Cooney
452 C. L., Evans J. M. B., Jamison T. F., Jensen K. F., Myerson A. S., Trout B. L., End-to-end
453 continuous manufacturing of pharmaceuticals: integrated synthesis, purification, and final dosage
454 formation, Angew. Chem. Int. Ed. Engl., 52: 12359-12363 (2013).

455 Melocchi A., Loreti G., Del Curto M. D., Maroni A., Gazzaniga A., Zema L., Evaluation of hot
456 melt extrusion and injection molding for continuous manufacturing of immediate release tablets, J.
457 Pharm. Sci., 104: 1971-1980 (2015a).

458 Melocchi A., Parietti F., Loreti G., Maroni A., Gazzaniga A., Zema L., 3D printing by fused
459 deposition modeling (FDM) of a swellable/erodible capsular device for oral pulsatile release of
460 drugs, J. Drug. Deliv. Sci. Technol., 30 Part B: 360-367 (2015b).

461 Norman J., Madurawe R. D., Moore C. M. V., Khan M. A., Khairuzzaman A., A new chapter in
462 pharmaceutical manufacturing: 3D-printed drug, Adv. Drug Deliv. Rev.,
463 doi:10.1016/j.addr.2016.03.001 (2016).

464 Park K., 3D printing of 5-drug polypill, J. Control. Release, 217: 352 (2015).

Pietrzak K., Isreb A., Alhnan M. A., A flexible-dose dispenser for immediate and extended release 3D printed tablets, Eur. J. Pharm. Biopharm., 96: 380-387 (2015).

Pham D. T., Gault R. S., A comparison of rapid prototyping technologies, Int. J. Mach. Tools Manuf., 38: 1257-1287 (1998).

Prasad L. K., Smyth H., 3D Printing technologies for drug delivery: a review, Drug Dev. Ind. Pharm., 13: 1-13 (2015).

Rengier F., Mehndiratta A., von Tengg-Kobligk H., Zechmann C. M., Unterhinninghofen R., Kauczor H. U., Giesel F. L., 3D printing based on imaging data: review of medical applications, Int. J. Comput. Assist. Radiol. Surg., 5: 335-341 (2010).

Sandler N., Salmela I., Fallarero A., Rosling A., Khajeheian M., Kolakovic R., Genina N., Nyman J., Vuorela P., Towards fabrication of 3D printed medical devices to prevent biofilm formation, Int. J. Pharm., 459: 62-64 (2014).

Sangalli M. E., Maroni A., Foppoli A., Zema L., Giordano F., Gazzaniga A., Different HPMC viscosity grades as coating agents for an oral time and/or site-controlled delivery system: a study on process parameters and in vitro performances, Eur. J. Pharm. Sci., 22: 469-476 (2004).

Sangalli M. E., Maroni A., Zema L., Cerea M., Gazzaniga A., The Chronotopic™ technology, in: B.-B.C. Youan (Ed.), Chronopharmaceutics. Science and technology for biological rhythm guided therapy and prevention of diseases, John Wiley&Sons, Hoboken, New Jersey, pp. 145-163 (2009).

Skowyra J., Pietrzak K., Alhnan M. A., Fabrication of extended-release patient-tailored prednisolone tablets via fused deposition modelling (FDM) 3D printing, Eur. J. Pharm. Sci., 68: 11-17 (2015).

Shah S., Maddineni S., Lu J., Repka M. A., Melt extrusion with poorly soluble drugs, Int. J. Pharm., 453: 233-52 (2013).

488 Water J. J., Bohr A., Boetker J., Aho J., Sandler N., Nielsen H. M., Rantanen J., Three-dimensional
489 printing of drug-eluting implants: preparation of an antimicrobial polylactide feedstock material, J.
490 Pharm. Sci., 104:1099-1107 (2015).

491 Yu D. G., Zhu L. M., Branford-White C. J., Yang X. L., Three-dimensional printing in
492 pharmaceutics: promises and problems, J. Pharm. Sci., 97: 3666-3690 (2008).

493 Zema L., Loreti G., Melocchi A., Maroni A., Gazzaniga A., Injection molding and its application to
494 drug delivery, J. Control. Release, 159: 324-331 (2012).

495 Zema L., Loreti G., Melocchi A., Maroni A., Palugan L., Gazzaniga A., Gastroresistant capsular
496 device prepared by injection molding, Int. J. Pharm., 440: 264-272 (2013b).

497 Zema L., Loreti G., Macchi E., Foppoli A., Maroni A., Gazzaniga A., Injection-molded capsular
498 device for oral pulsatile release: development of a novel mold, J. Pharm. Sci., 102: 489-499
499 (2013a).

**Table(s)**

**Table 1:** weight and thickness of PLA disks fabricated after 3 leveling of the build plate by 2 different operators

| | **Leveling replicate** | **Weight** mg (CV) *n = 6* | **Thickness** µm (CV) | | | |
|---|---|---|---|---|---|---|
| | | | Outer circumference *n = 6* | Intermediate circumference *n = 6* | Inner circumference *n = 6* | All circumferences *n = 18* |
| **Operator 1** | I | 514.6 (1.7) | 636 (4.1) | 626 (5.1) | 622 (5.2) | 628 (4.8) |
| | II | 514.4 (0.5) | 680 (5.6) | 665 (4.6) | 673 (6.6) | 673 (5.6) |
| | III | 520.9 (0.2) | 720 (8.0) | 706 (5.6) | 724 (8.9) | 717 (7.6) |
| **Operator 2** | I | 507.5 (1.3) | 643 (6.9) | 633 (4.7) | 635 (5.6) | 637 (5.7) |
| | II | 525.4 (0.2) | 737 (5.0) | 736 (6.3) | 739 (3.6) | 738 (4.9) |
| | III | 533.9 (0.2) | 844 (8.9) | 838 (7.2) | 832 (7.2) | 832 (7.8) |
| **All leveling replicates *n = 36*** | | **519.5 (1.8)** | **710 (12.0)** | **701 (11.8)** | **701 (11.0)** | **704 (11.7)** |

**Table 2:** formulation, process parameters and photographs relevant to extruded filaments and printed disks (entire and magnified detail) based on different pharmaceutical grade polymers

| FORMULATION | HME | | | | FDM | | |
|---|---|---|---|---|---|---|---|
| | T (°C) | Screw speed (rpm) | Torque (N·cm) | Product ⊢⊣ 5 mm | T (°C) | Product ⊢⊣ 10 mm | Product x 10 magnification |
| **KIR + 12% GLY** | 160 | 100 | 80 |  | 180 |  | 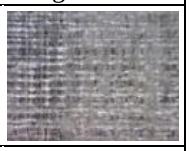 |
| **PEO** | 65 | 100 | 100 | 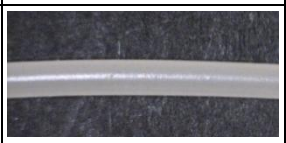 | 160 | 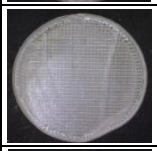 |  |
| **HPMC + 5% PEG 400** | 160 | 70 | 70 |  | 200 | 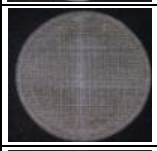 | 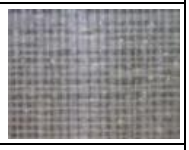 |
| **HPC** | 165 | 80 | 40 |  | 180 |  | 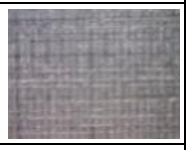 |
| **PVA+ 5% GLY** | 190 | 70 | 80 |  | 225 |  | 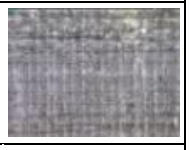 |
| **SLP + 10% PEG 400** | 120 | 80 | 80 | 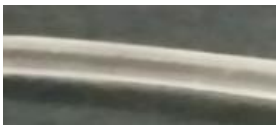 | 200 |  |  |
| **HPMCAS + 5% PEG 8000** | 180 | 100 | 100 |  | 200 | 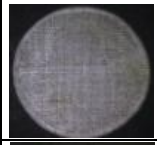 |  |
| **EDR L + 20% TEC** | 160 | 80 | 120 |  | 160 |  |  |
| **EDR RL + 15% TEC** | 120 | 95 | 60 |  | 160 |  |  |
| **EC + 10% TEC** | 160 | 100 | 100 |  | 200 | 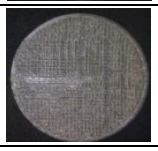 | 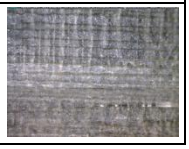 |

**Table(s)**

**Table 3:** weight and thickness data of printed disks based on different pharmaceutical grade polymers

| **FORMULATION** | **Weight** mg (CV) | **Thickness** µm (CV) | | | |
|---|---|---|---|---|---|
| | | Outer circumference *n = 6* | Intermediate circumference *n = 6* | Inner circumference *n = 6* | All circumferences *n = 18* |
| **KIR + 12% GLY** | 477.4 (3.8) | 634 (9.2) | 601 (5.7) | 623 (7.6) | 614 (7.5) |
| **PEO** | 364.0 (12.8) | 571 (10.6) | 563 (11.2) | 555 (14.0) | 563 (11.9) |
| **HPMC + 5% PEG 400** | 435.7 (9.2) | 605 (12.8) | 559 (10.7) | 526 (12.7) | 563 (11.4) |
| **HPC** | 423.3 (2.0) | 645 (5.9) | 635 (6.2) | 634 (5.2) | 638 (5.8) |
| **PVA+ 5% GLY** | 352.0 (10.3) | 528 (8.9) | 545 (12.8) | 527 (6.5) | 533 (9.9) |
| **SLP + 10% PEG 400** | 325.0 (13.6) | 543 (18.0) | 540 (17.1) | 528 (21.6) | 537 (18.8) |
| **HPMCAS + 5% PEG 8000** | 373.5 (5.8) | 504 (11.8) | 479 (15.0) | 450 (12.9) | 478 (13.9) |
| **EDR L + 20% TEC** | 354.0 (9.0) | 486 (14.6) | 474 (13.5) | 468 (11.6) | 476 (13.4) |
| **EDR RL + 15% TEC** | 336.9(5.9) | 660 (13.1) | 660 (11.9) | 683 (10.1) | 668 (11.8) |
| **EC + 10% TEC** | 442.7 (4.8) | 629 (6.1) | 620 (5.9) | 623 (5.8) | 624 (5.9) |

**Table(s)**

**Table 4:** TETP from disks based on swellable/erodible polymers

| **FORMULATION** | **TETP** μm/min (CV) |
|---|---|
| HPMC + 5% PEG 400 | 7.36 (0.33) |
| SLP + 10% PEG 400 | 15.54 (2.28) |
| HPC | 22.42 (4.17) |
| PVA + 5% GLY | 37.84 (2.05) |

**Figure 1:** image of a printed disk reporting the 3 concentric circumferences along which thickness was measured (outer circumference, white; intermediate circumference, grey; inner circumference, black)

**Figure 2:** test cells before assembly (a) and after filling of the reservoir donor compartment with AAP powder (b), positioning of the disk (c) and final assembly (d)

**Figure 3:** drug recovered *vs* time profiles obtained from disks based on promptly soluble polymers

**Figure 4:** individual drug recovered *vs* time profiles obtained from disks based on HPMC

**Figure 5:** drug recovered *vs* time profiles obtained from disks based on insoluble polymers

**Figure 6:** drug recovered *vs* time profiles obtained from single (a) and double (b) disks containing furosemide; lateral views of disks are also reported

**Figure(s)**

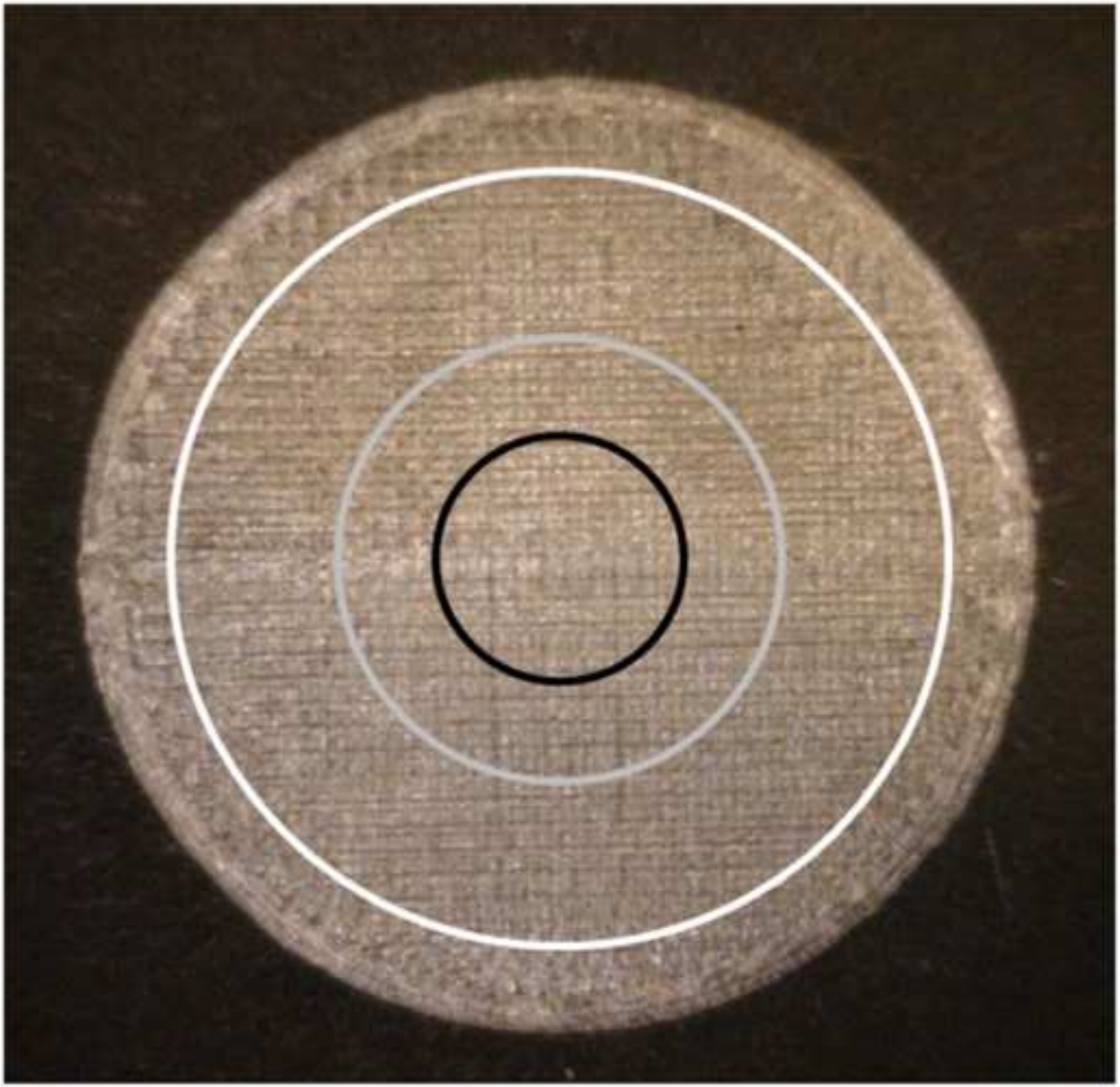

**Figure(s)**

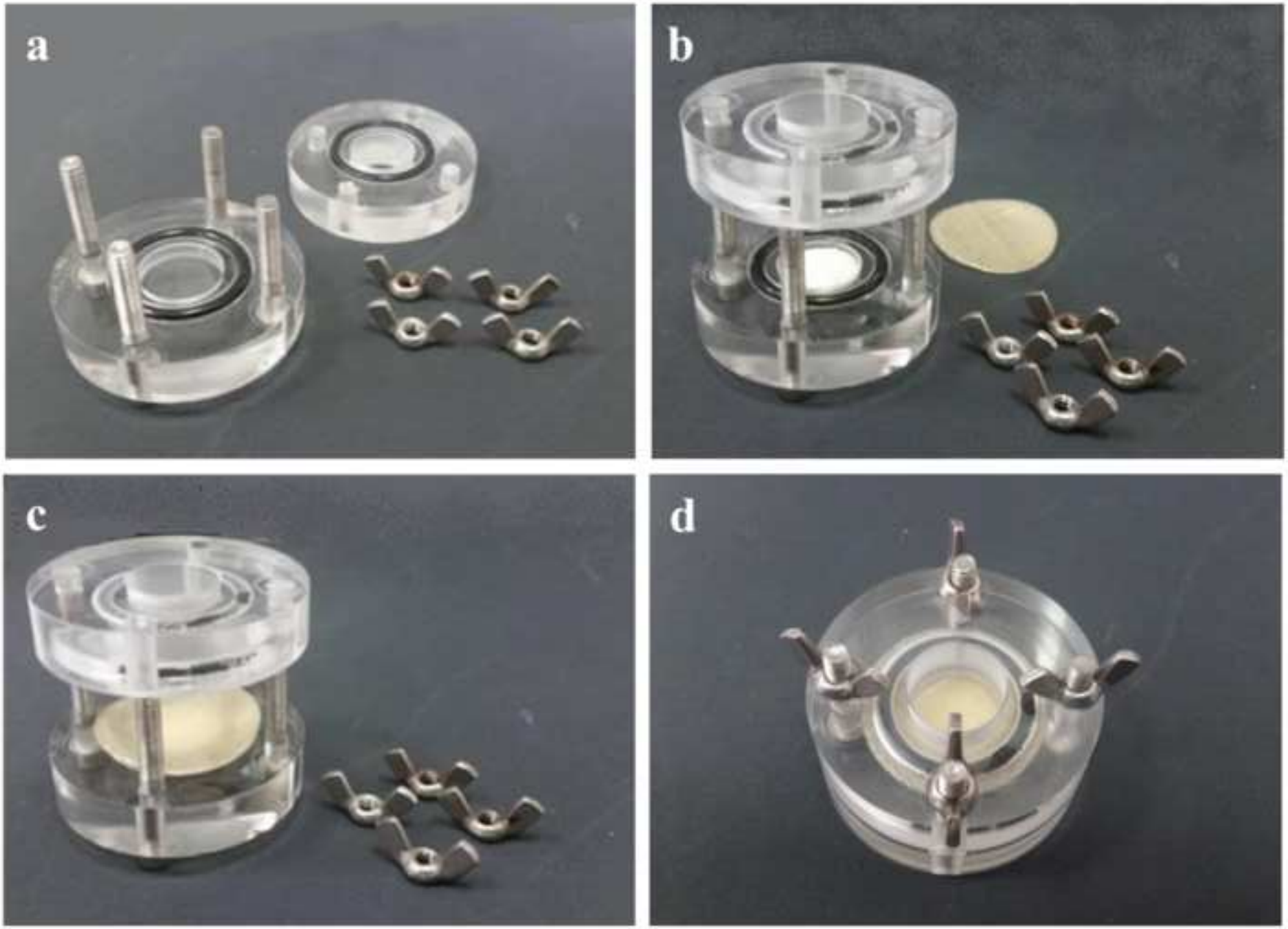

Figure(s)

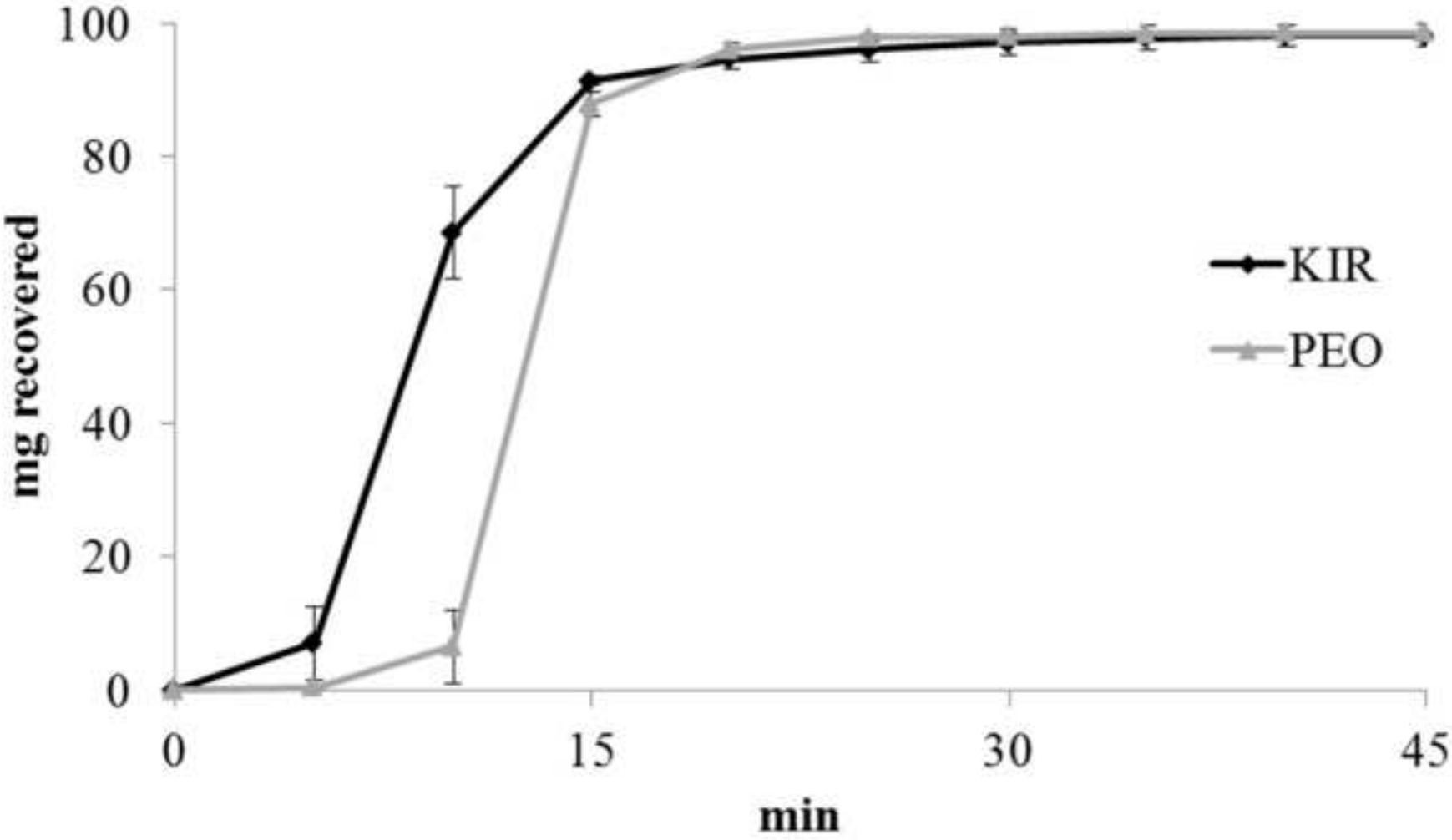

Figure(s)

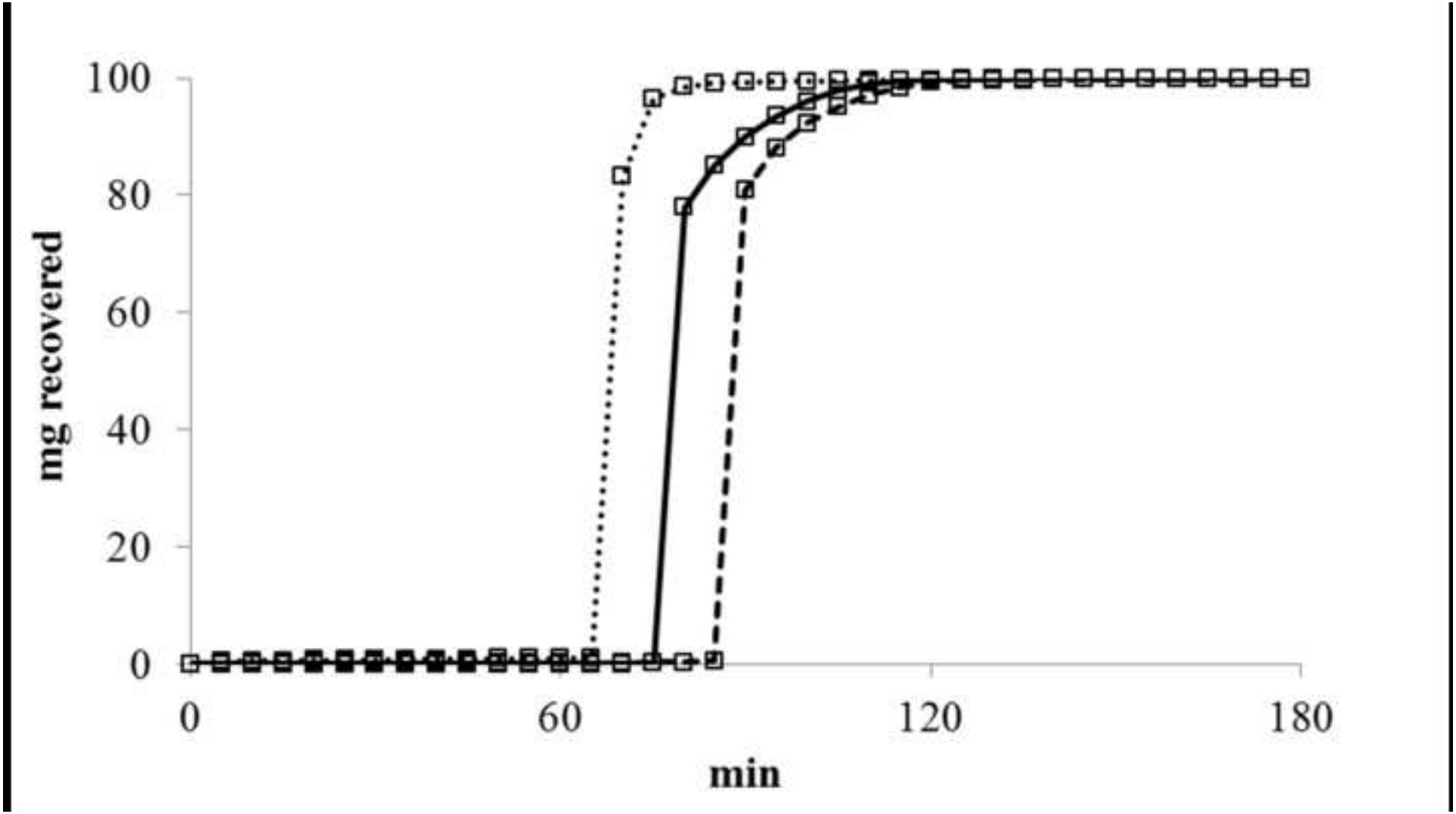

Figure(s)

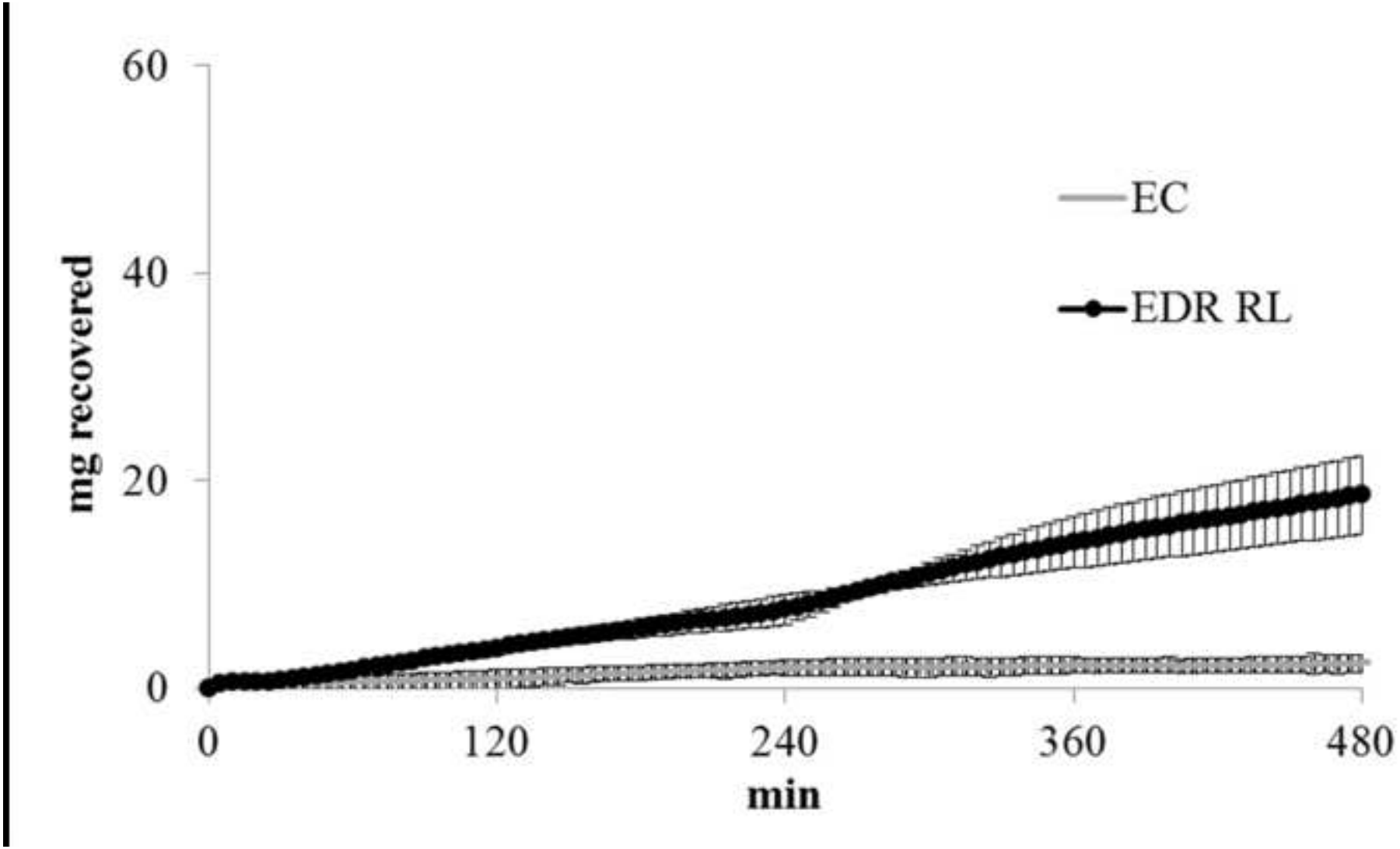

Figure(s)

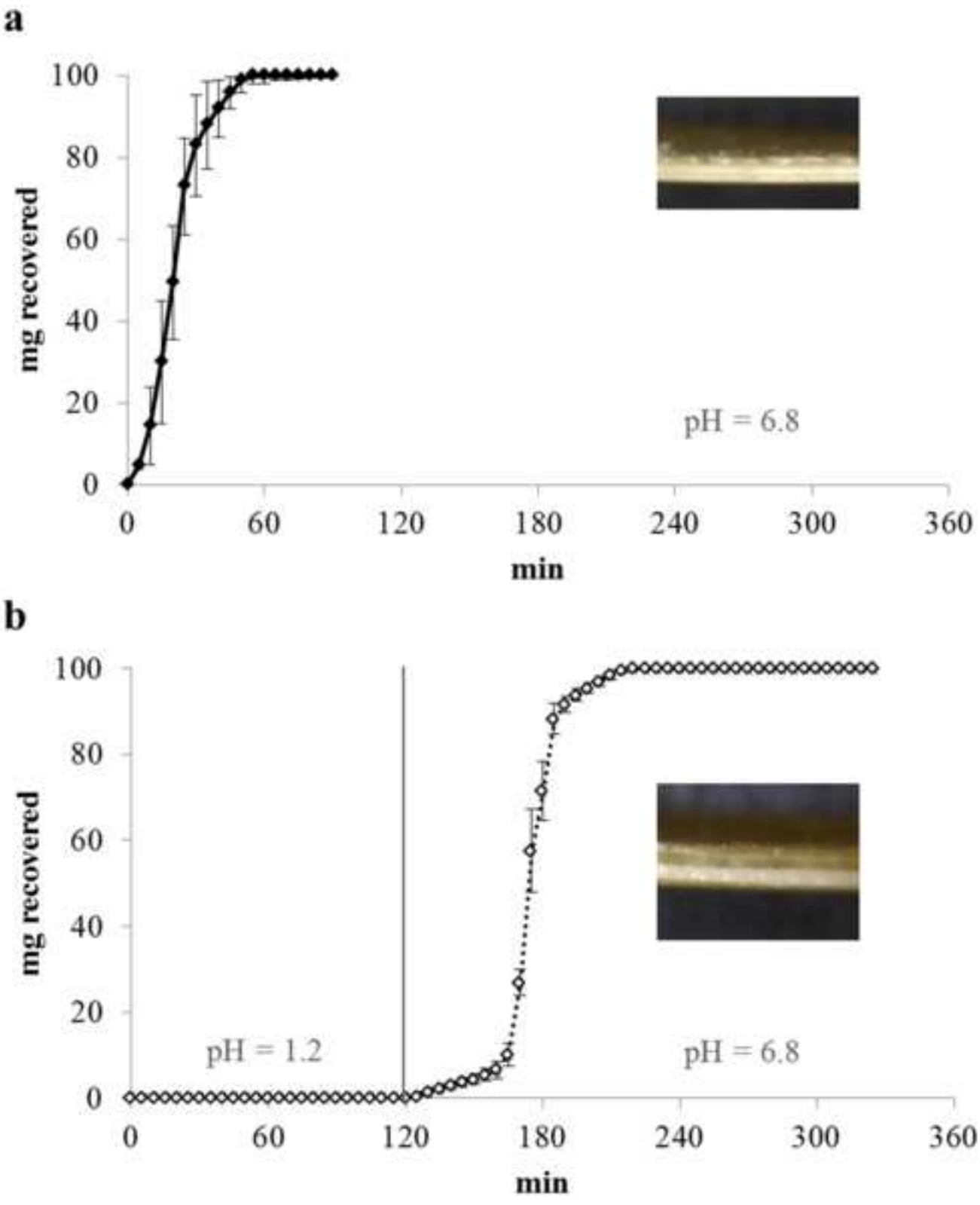
a
100
80
60
40
20
0
mg recovered
pH = 6.8
0
60
120
180
240
300
360
min
b
100
80
60
40
20
0
mg recovered
pH = 1.2
pH = 6.8
0
60
120
180
240
300
360
min